

4,6-Dimethyl-2-Oxo-1,2-Dihydro-pyridine-3-Carboxylic Acid as an Inhibitor Towards the Corrosion of C-Steel in Acetic Acid

S. Abd El Wanees^{1, 2, *}, Mohamed I. Alahmdi², M. Abd El Azzem³ and Hamdy E. Ahmed⁴

¹ Chemistry Department, Faculty of Science, Zagazig University, Zagazig 44519, Egypt

² Chemistry Department, Faculty of Science, University of Tabuk, Tabuk, Kingdom of Saudi Arabia

³ Department of Chemistry, Faculty of Science, Monufia University, Monufia, Egypt

⁴ Lab Section Head, Khalda Petroleum Company, Egypt

E-mail: s_wanees@yahoo.com

Received: 27 January 2016 / Accepted: 28 February 2016 / Published: 1 April 2016

The effect of 4,6-dimethyl-2-oxo-1,2-dihydro-pyridine-3-carboxylic acid (DODHPCA) as a corrosion inhibitor for C-steel in acetic acid is examined by using hydrogen gas evolution, mass loss and potentiodynamic polarization techniques, as well as SEM investigation. Results showed that, the compound under study exhibits inhibitor properties. The inhibition efficiency was found to depend on the inhibitor concentration. The inhibition effect is based on the adsorption of DODHPCA molecules on the metal surface following Langmuir adsorption model. Tafel polarization curves indicated that this compound was of a mixed-type. The thermodynamic parameters are calculated and discussed.

Keywords: Corrosion, C-Steel, Acetic acid, Inhibitor

1. INTRODUCTION

Many scientists had sustained a great effort to study the corrosion processes and the behavior of carbon steel used in oil and gas pipelines in order to find suitable corrosion inhibitors and preservation of mineral wealth [1-6]. Multiple stages systems, which contain brine and acetic acid, lead to a significant increase in the corrosion of carbon steel operations. Acetic acid is an organic acid that causes type of localized corrosion on carbon steel by removing the iron carbonate layer, which formed when the metal surface is exposed to an aqueous solution [7]. The electrochemical impedance spectroscopic studies indicate that the surface cathodic reactions were enhanced in the presence of acetic acid [8] due to the reduction of un-dissociated acetic acid with a subsequent increase in the anodic current density [9].

The presence of some organic molecules containing hetero atoms reduces the corrosion of metallic materials (when added to the aggressive acidic solutions) [10]. These materials are added in very small quantities in order to reduce or discouraged the corrosion processes [10, 11]. They will reduce, slow down or prevent the corrosion process of the metal in aqueous solution. The selection of the effective inhibitor takes great attention of several investigators [10-12]. The selection of inhibitors is based on the experimental methods for metal protection against corrosion and depends on many factors among of which are the metals or alloys to be protected, as well as the severity of the corrosive environment [10-19].

Generally, good inhibitors adsorb on the metal surface forming an insulating film that prevents the metal film from the corrosive solution and reduces the corrosion process [20]. The adsorption of the inhibitor on the metal surface is a complex process involving a number of factors such as the nature of the metal, the environment, the electrochemical potential at the metal/ solution interface and nature of the inhibitor [20]. Once adsorption of inhibitor molecule is started on the metal surface in aqueous phase, H₂O molecules are replaced.

The aim of the present work is to investigate the effect of 4,6-dimethyl-2-oxo-1,2-dihydropyridine-3-carboxylic acid (DODHPCA) as an inhibitor towards the corrosion of C-steel in CH₃COOH, using hydrogen gas evolution, mass loss and potentiodynamic polarization techniques. The adsorption mechanism and inhibition efficiency of the inhibitor are investigated and some thermodynamic parameters in absence and presence of the inhibitor are calculated and discussed [20].

2. MATERIALS AND METHODS.

2.1. Materials

The molecular structure and molecular formula of DODHPCA as an inhibitor are indicated in Table 1. The steel electrodes were made from steel samples produced by the Egyptian Steel Mill Company (Helwan–Cairo) and have the following chemical composition [21]:

C	Si	Mn	P	S	Fe
0.32	0.24	0.89	0.024	0.019	Bal 98.507 mass%

The electrode used for potentiodynamic polarization measurements was fixed to a borosilicate glass tube with epoxy resin so that the total exposed surface area is 0.5 cm². On the other hand, steel sheets with dimension 2 cm, 4 cm and 0.3 cm were used for mass loss and hydrogen evolution techniques. The samples and electrodes were prepared, abraded and cleaned as illustrated previously [21].

Table 1. Molecular structure and molecular formula of the inhibitor [22].

Name	Molecular structure	Molecular weight
4,6-Dimethyl-2-oxo-1,2-dihydropyridine-3-carboxylic acid (DODHPCA).		$C_8H_9NO_3 = 167$

2.2. Hydrogen evolution measurements

The procedure for the evolved H_2 gas on C-steel was carried out in glass container containing 100 ml of 3M CH_3COOH containing different concentrations of DODHPCA are described elsewhere [23]. The values of the surface coverage, θ and the inhibition efficiency, η % were calculated from the corrosion rate in absence and presence of inhibitor, according to equations 1 and 2, respectively [23].

$$\theta = \left[1 - \left(\frac{r'_{corr}}{r^o_{corr}} \right) \right] \quad (1)$$

$$\eta \% = \left[1 - \left(\frac{r'_{corr}}{r^o_{corr}} \right) \right] 100 \quad (2)$$

where r'_{corr} and r^o_{corr} are the rates of reaction of C-steel with and without DODHPCA, respectively.

2.3. Mass loss measurements

For mass loss measurements, a cleaned C-steel coupon was weighed before and after immersion in the test solution for a definite period, as shown before [23]. The average mass loss for each two identical experiments was taken and expressed in mg/cm^2 . The rate of corrosion, r_{corr} , in $mg/cm^2/min$ was determined from the relation:

$$r_{corr} = \frac{W}{(A t)} \quad (3)$$

where W is the loss in the sample weight, A is the sample surface area in cm^2 and t is the immersion time in min.

2.4. Potentiodynamic polarization measurements

The electrolytic cell, electrodes and the procedure used for polarization measurements were described previously [23-25]. Before carrying polarization, the steel electrode was subjected to cathodic pretreatment for 20 minutes in the test solution at -1.5V (SCE) to reduce any overlying oxide films that would be formed on the metal surface. Electrochemical polarization was made using a Potentiostat Type POS 73 (Germany), at a scan rate of 1mV/s [25].

2.5. Scanning Electron Microscope

Scanning electron microscope is used to investigate the corroded samples after immersion in the absence and presence of inhibitor. The surface investigation using SEM Model, Philips XL 30 equipped with EDX unit, with accelerating voltage of 30 KV, magnification up to 400,000 x, and resolution for W 3.5 nm.

3. RESULTS AND DISCUSSION

3.1. Hydrogen evolution measurements

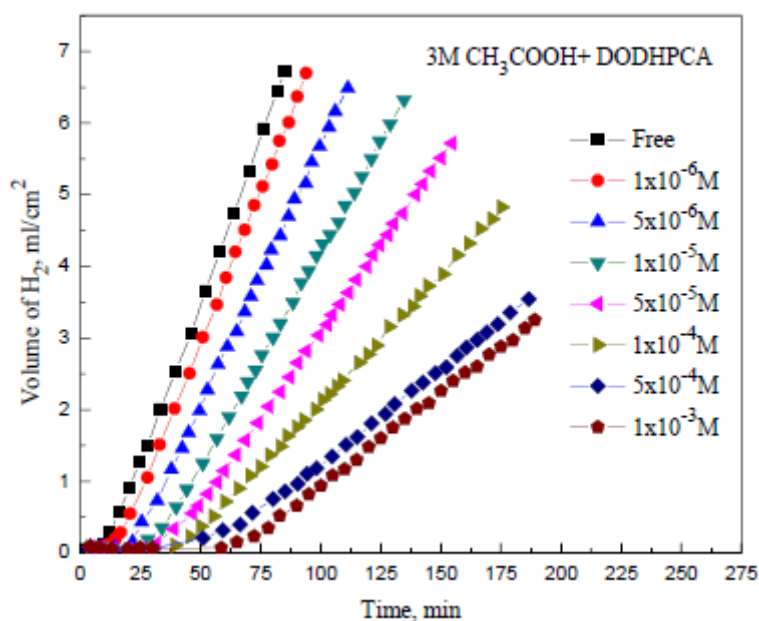


Figure 1. Variation of the volume of H₂ gas with the immersion time, for C-steel in 3M CH₃COOH solutions containing DODHPCA, at 25°C.

The corrosion behavior of C-steel in 3M CH₃COOH devoid of and containing different concentrations of the organic additive is examined. DODHPCA was added as an inhibitor in different concentrations to decrease the rate of corrosion of C-steel in 3M CH₃COOH solutions by gasometry method.

The data of Fig 1 illustrate the volume-time change for the evolved hydrogen gas on C-steel surface in 3M CH₃COOH containing different concentrations of the organic additive. Inspection of these curves reveals that evolved hydrogen gas starts after the elapses of a certain time from the immersion of steel sample in the test solution, incubation period, τ . This period is found to depend on the inhibitor concentration and temperature [23]. After the induction period, the curves in this figure are characterized by linear variation of the volume of the evolved hydrogen gas with time. The values of the corrosion rates, r'_{corr} , obtained from the slope of the linear parts of volume-time plots for the test solutions [23] are shown in Table 2.

Table 2. Corrosion parameters data for C-steel in CH₃COOH containing gradient concentrations of DODHPCA inhibitor, at 25°C.

Concentration, M	Gasometry method			Mass loss method		
	r'_{corr} , cm min ⁻¹	θ	η %	r_{corr} , $\mu\text{g}/\text{cm}^2/\text{min}$	θ	η %
Blank	0.0911	-	-	23.80	--	--
1.0 x10 ⁻⁶ M	0.0851	0.066	65.8	--	--	--
5.0 x10 ⁻⁶ M	0.0726	0.203	20.3	21.18	0.110	11.0
1.0 x10 ⁻⁵ M	0.0607	0.333	33.3	19.49	0.181	18.1
5.0 x10 ⁻⁵ M	0.0486	0.466	46.3	12.61	0.470	47.0
1.0 x10 ⁻⁴ M	0.0408	0.552	55.2	9.00	0.622	62.2
5.0 x10 ⁻⁴ M	0.0268	0.668	66.8	5.38	0.774	77.4
1.0 x10 ⁻³ M	0.0250	0.726	72.6	4.69	0.803	80.3

The data indicate that, presence of inhibitor in 3M CH₃COOH solution decreases the reaction rate of C-steel. Fig 2 (A) show the variation in the rate of dissolution reaction, r'_{corr} of C-steel in 3M CH₃COOH solution with DODHPCA concentration. The dissolution reaction rate, r'_{corr} , varies with the inhibitor, C_{inh} , according the relation [26]:

$$\log r'_{\text{corr}} = k' - B' \log C_{\text{inh}} \tag{4}$$

where k' and B' are constants. The effect of additions of DODHPCA on the reduction of the corrosion reaction (rate of production of H₂ gas), r'_{corr} was related to the inhibitor concentration, as shown in Table 2. The values of θ and η % in presence of different concentrations of DODHPCA are calculated from the corrosion rate values according to equations 1 and 2, respectively, Table 2.

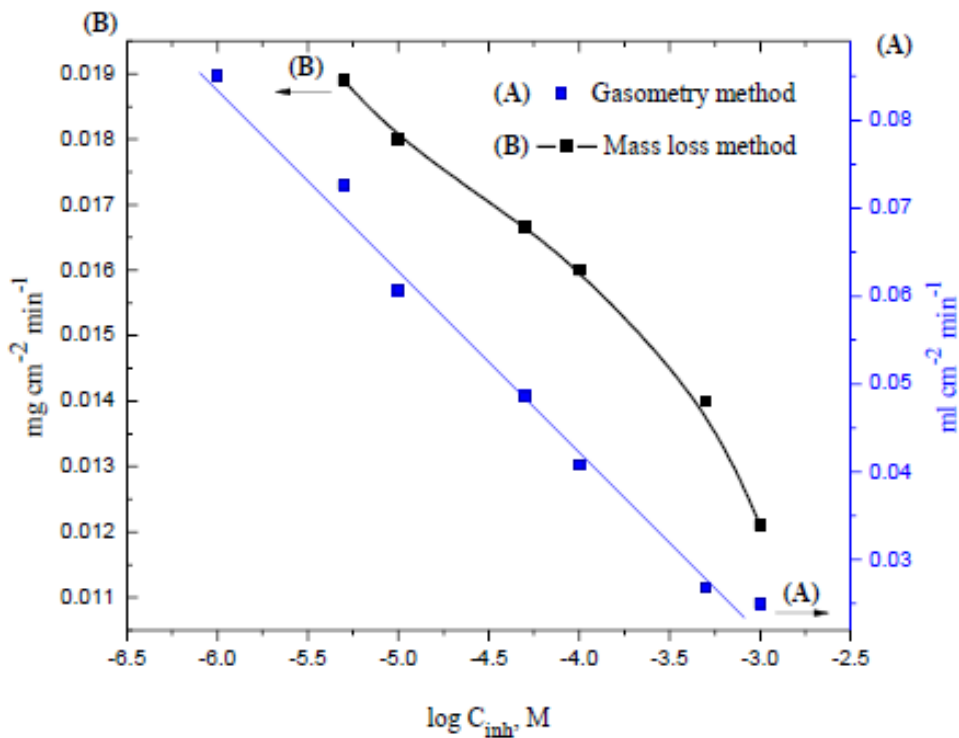


Figure 2. Variation of the rate of corrosion reaction in CH₃COOH with DODHPCA concentration.

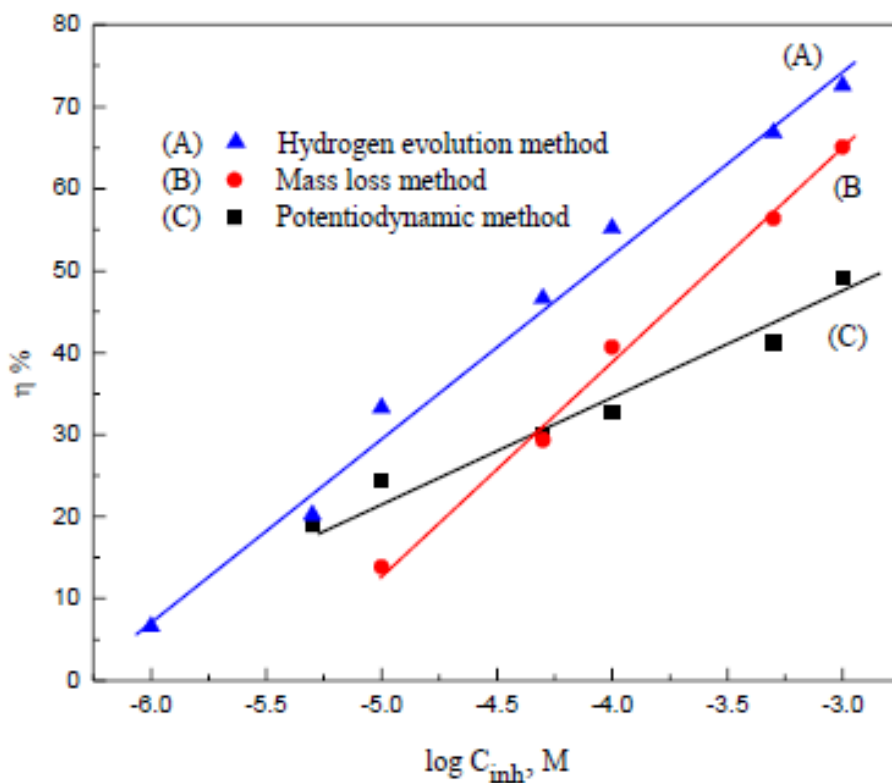


Figure 3. Variation of the inhibition efficiency, $\eta\ %$ with the logarithm of DODHPCA concentration.

3.2. Mass loss Measurements

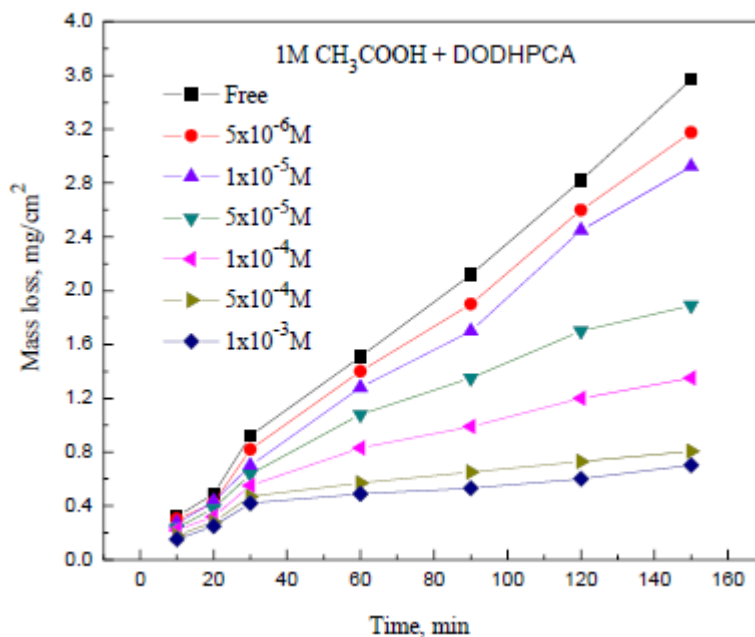


Figure 4. Mass loss- time plots of C-steel in 1M CH₃COOH with and without different concentrations of DODHPCA.

Fig 3(A) shows the variation of the inhibition efficiency, $\eta\%$ of organic additive with the logarithm of the inhibitor concentration. From the plots of this figure, as well as, the data of Table 2, the values of each of θ and $\eta\%$ were found to depend on the inhibitor concentration. These values are increased by increasing inhibitor concentration. It is noteworthy to see that, the variation of θ with inhibitor concentration is proved to follow Langmuir's adsorption isotherm as will be discussed later.

Fig 4 shows the variation in the mass loss of the C-steel coupons (ΔW , mg cm⁻²) in 1M CH₃COOH solutions devoid of and containing different concentrations of DODHPCA, with the immersion time, at 25°C. The plots clearly illustrate the corrosion susceptibility of the C-steel sample in the absence and presence of the inhibitor. The loss in mass due to corrosion of the C-steel coupons with the free acid solution was higher than that in presence of the inhibitor. It is important to note that the data of the corrosion rate expressed in mg cm⁻² min⁻¹ of C-steel in 1M CH₃COOH solution can be plotted against the inhibitor concentration on a double logarithmic scale, Fig 2 (B). The S-shaped curve of Fig 2 (B) recognize the suppression of the dissolution process initiated by the specific adsorption of the inhibitor molecules on the C-steel surface [23, 25, 27]. The data of this figure, as well as the data of Table 2 indicate that the inhibition efficiency of DODHPCA towards corrosion process increases with inhibitor concentration.

Generally, it is accepted that the adsorption of the organic inhibitor on the metal surface represents the most important action that retards the dissolution reaction. The extent and mode of the adsorption depends on the molecule's chemical composition, the temperature and the electrochemical potential at the metal/solution interface. In fact, the solvent H₂O molecules could also adsorb at

metal/solution interface. So, the adsorption of organic inhibitor molecules from the aqueous solution can be regarded as a quasi-substitution process between the organic compound in the aqueous phase, $Org_{(sol)}$, and water molecules at the electrode surface [27, 28]. The adsorption extent also depends on the metal surface and the electrolyte concentration.

The surface coverage, θ and the inhibition efficiency, $\eta\%$, of the organic compound were calculated using the following equations[27, 29, 30]:

$$\theta = \frac{r^{\circ} - r}{r^{\circ}} \tag{5}$$

$$\eta \% = \left(\frac{r^{\circ} - r}{r^{\circ}} \right) 100 \tag{6}$$

where r° and r are the corrosion rates in the absence and presence of inhibitor, respectively. Each of surface coverage, θ and the inhibition efficiency, η %, increases as the inhibitor concentration is increased, Table 2. Fig 3(B) represents the variation of the inhibition efficiency, η %, with the logarithm of inhibitor concentration. A straight-line relation is obtained confirming the direct relation between the inhibition efficiency and the inhibitor concentration.

3.3. Potentiodynamic Polarization

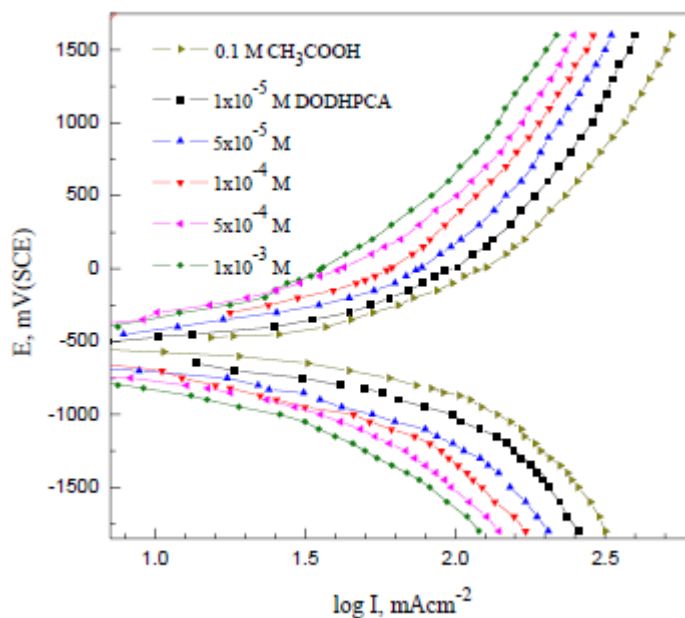


Figure 5. Anodic- cathodic potentiodynamic polarization curves of C-steel in 0.1 M CH_3COOH devoid of and containing different concentrations of DODHPCA.

The potentiodynamic polarization behavior of C-steel in 0.1M CH_3COOH solution devoid of and containing different concentrations of DODHPCA was also investigated. Fig 5 shows the E - $\log I$ curves of C-steel in 0.1M CH_3COOH solution with and without different concentrations of DODHPCA. It is noted that, as the inhibitor concentration is increased the polarization curves are shifted into more negative values and more positive values, successively, with cathodic and anodic

reactions. The results suggest that the DODHPCA additive acts as cathodic and anodic inhibitor (mixed-type inhibitor) [31]. Also, the anodic Tafel slopes, $b_a = 453 \pm 5$ mV/decade, (mean value 457 mV/decade) and the cathodic Tafel slopes, $b_c = 684 \pm 5$ mV/decade, (mean value 588 mV/decade) did not change appreciably upon adding the studied organic inhibitor, DODHPCA (as shown in Table 3).

Table 3. Electrochemical corrosion parameters, E_{corr} , mV(SCE), i_{corr} , mAcm⁻², b_a , mV/decade, b_c , mV/decade, θ and η %, for C-steel in 0.1M CH₃COOH in the absence and presence of different concentrations of DODHPCA, at 25°C.

Solution	E_{corr} , mV (SCE)	i_{corr} , mAcm ⁻²	b_a , mV/decade	b_c , mV/decade	θ	η %
Free	-526	45.85	453	684	--	--
1x10 ⁻⁵ M	-555	39.50	455	688	0.138	13.80
5x10 ⁻⁵ M	-565	32.40	458	689	0.293	29.30
1x10 ⁻⁴ M	-573	25.22	457	690	0.407	40.65
5x10 ⁻⁴ M	-580	20.00	459	691	0.564	56.40
1x10 ⁻³ M	-698	16.00	460	686	0.651	65.10

The convergence in the values of each of b_a and b_c Tafel slopes confirm that, the presence of DODHPCA compound with CH₃COOH does not affect the mechanism of anodic nor the cathodic reactions, even though it significantly reduce its rate [32]. The shift in both anodic and the cathodic Tafel slopes in presence of such compound, suggest that, the inhibition action of DODHPCA occurs by simple blocking of the electrode surface through adsorption [23, 33]. It is noteworthy to see that the calculated corrosion current density, i_{corr} , decreases as the inhibitor concentration is increased, (Fig 6 & Table 3).

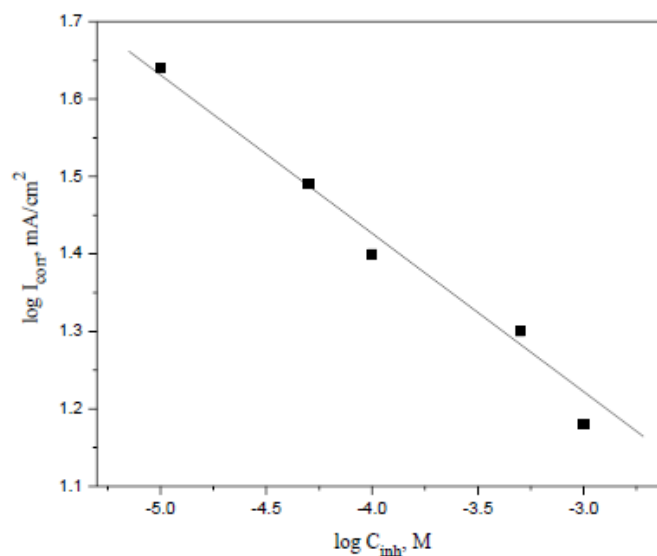


Figure 6. Variation of the corrosion current density of C-steel in 0.1 M CH₃COOH with the inhibitor concentration

The surface coverage, θ , and the inhibition efficiency, η % included in Table 3 were calculated according to the following equations [31-33]:

$$\theta = \left[1 - \left(\frac{i_{corr,inh}}{i_{corr,free}} \right) \right] \quad (7)$$

$$\eta \% = \left[1 - \left(\frac{i_{corr,inh}}{i_{corr,free}} \right) \right] 100 \quad (8)$$

where $i_{corr,free}$ and $i_{corr,inh}$ are the corrosion current densities of C-steel in the absence and presence of inhibitor, respectively. It is observed that the inhibition efficiency, η % increases with increasing the inhibitor concentration. The increase in the η % with DODHPCA concentration could be attributed to the bond formed between the organic compound and the bare metal surface [23]. This bond is mainly accompanied with the existence of electron densities enriched with the available adsorption centers involved in the inhibitor molecule [22]. The studied compound has more than adsorption center, like N, O and the π -electrons of conjugated system of the molecule. So, the presence of DODHPCA in corrosion system will enhances the inhibition process, and tolerates the corrosive effect of acetic acid [22].

3.4. Effect of temperature

The effect of temperature is studied on the corrosion rate for C-steel in 1M CH₃COOH with and without 1×10^{-4} M DODHPCA using mass loss method. The activation energies of the corrosion reaction is calculated with and without DODHPCA [23, 35]. This was completed by studying the temperature effect on C-steel devoid of (Fig. 7) and containing of 1×10^{-4} M inhibitor (Fig. 8).

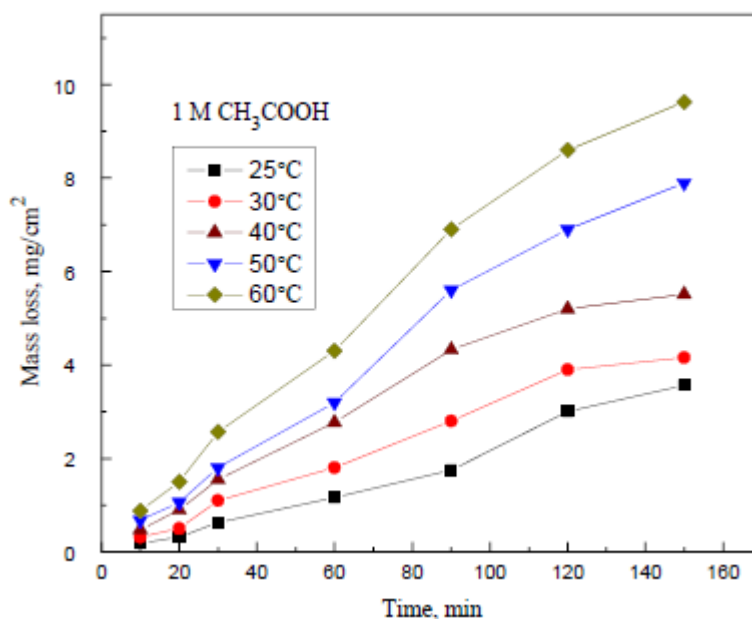


Figure 7. Variation of mass loss with time for C-steel in 1M CH₃COOH at different temperatures.

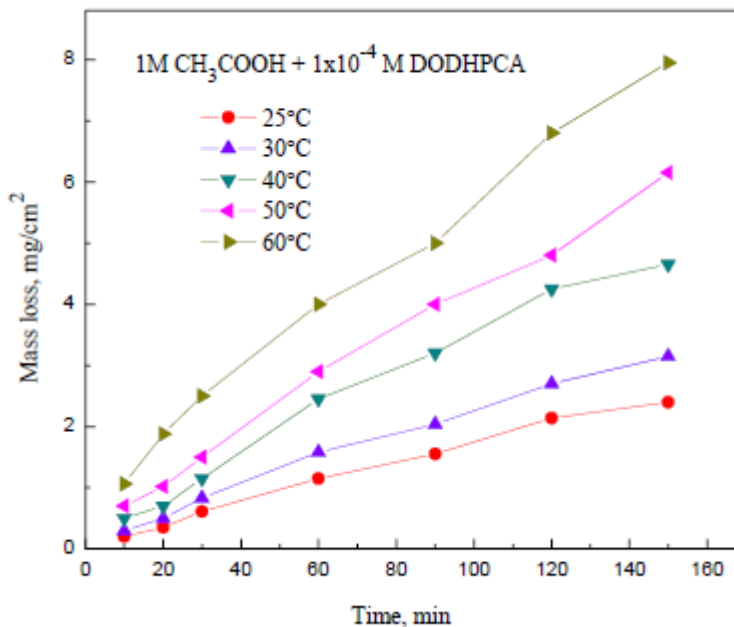


Figure 8. Variation of mass loss with time for C-steel in 1M CH₃COOH containing 1x10⁻⁴M DODHPCA, at different temperatures.

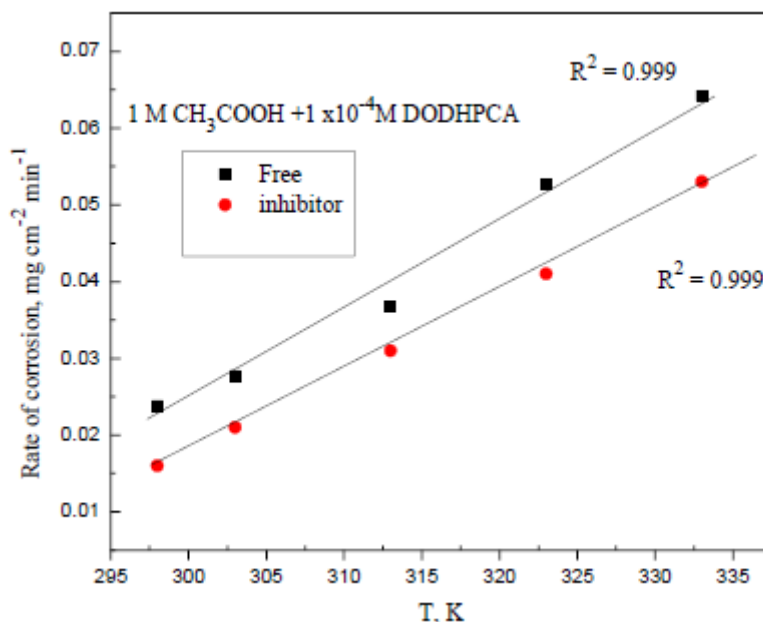


Figure 9. Variation of the rate of corrosion with temperature for C-steel in 1M CH₃COOH devoid of and containing 1 x10⁻⁴M inhibitor.

It is clear that, in the absence and presence of inhibitor, the rate of corrosion increases directly with temperature. The variation of the rate of corrosion with the absolute temperature (T), Fig 9, follows the relation:

$$\log r = a + b T \tag{9}$$

where a and b are constants which depend on the solution concentration and metal under test, Table 4.

Table 4. Values of the constants *a* and *b* of equation 9.

1 M CH ₃ COOH+1x10 ⁻⁴ M DODHPCA	<i>a</i> , μg/cm ² /min	<i>b</i> , μg/cm ² /min/decade
Free	-3.3 x10 ⁻¹	11.8x10 ⁻⁴
Inhibitor	-3.0 x10 ⁻¹	10.5x10 ⁻⁴

The constant *a* represents the rate of corrosion of steel at zero Kelvin. It is clear that the rate of corrosion increases as the temperature is increased, both in absence and in presence of inhibitor. In addition, the convergence in values of the constant *b*, in case of free acid and inhibitor indicates that the mechanism of corrosion of C-steel in the absence and presence of inhibitor is the same and is not influenced by presence of inhibitor, despite the reduction in the corrosion rate.

For further insight on the mechanism of temperature on the rate of reaction of C-steel. The adoption of the rate of reaction, *r*, on temperature can be expressed by Arrhenius relation[36]:

$$r = A \exp \left(\frac{-\Delta E_a}{RT} \right) \tag{10}$$

where *A* is the Arrhenius constant, Δ*E_a*, is the activation energy of the metal corrosion reaction, *R* is the universal gas constant. Rearranging equation (10) gives[36]:

$$\log r = \log A - \frac{\Delta E_a}{2.303RT} \tag{11}$$

The dependence of log *r* on 1/*T* for C-steel in 1M CH₃COOH devoid of and containing 1x10⁻⁴ M of DODHPCA are plotted in Fig 10.

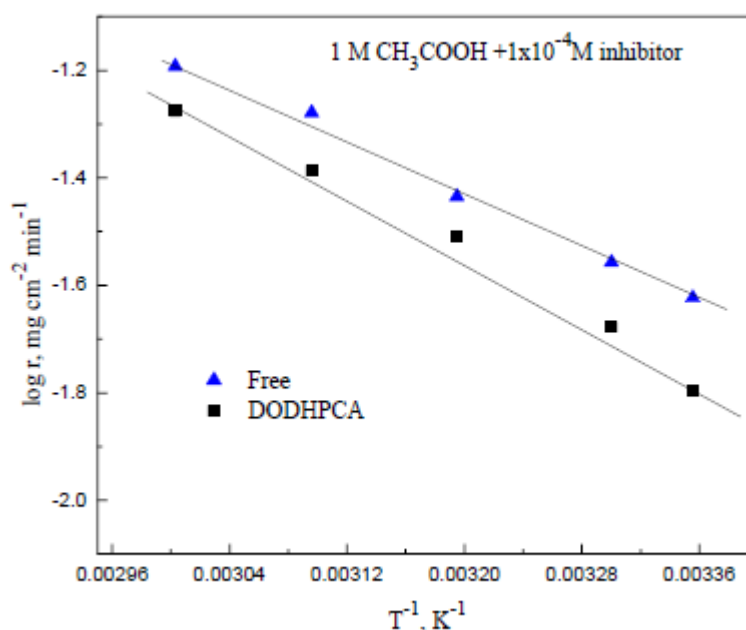


Figure 10. Arrhenius plots for C-steel in 1M CH₃COOH devoid of and containing 1x10⁻⁴ M inhibitor.

Linear plots are obtained which indicates that it follows Arrhenius equation. The Δ*E_a* values are calculated from the slope values of the linear plots, and are shown in Table 5.

Table 5. Thermodynamic parameters, ΔE_a , ΔH_a and ΔS_a for corrosion of C-steel in 1M CH₃COOH devoid of and containing 1x10⁻⁴ M inhibitor.

Solution	ΔE_a , kJ/mole	ΔH_a , kJ/mole	ΔS_a , J/mole	K_{ads} , M ⁻¹	ΔG°_{ads} , kJ/mole
Free	24.01	19.91	-209	--	--
Inhibitor	27.80	25.20	-194	23513	34.88

The higher value of ΔE_a in case of the additive compared to that of blank is indicative in a decrease in the dissolution rate of C-steel in the acid due to an increase in energy barrier layer resulted from adsorption of the inhibitor on steel surface [37, 38].

Many researchers attributed the decrease in ΔE_a values in presence of inhibitor compared to blank to the chemical reaction between inhibitor and the metal under diffusion-controlled process. From the other point of view of literature, the lower values of ΔE_a for corrosion in solutions containing inhibitor would be accompanied by a chemisorption step, which was the opposite of physical adsorption [2, 38]. The calculated value of ΔE_a in case of DODHPCA was higher than that of free acid. This is consider as an indication that physic-sorption process predominates with DODHPCA. It is also considered as a confirmation that the inhibition process is controlled by surface reaction, since the values of ΔE_a of the corrosion process are above 20 kJ mol⁻¹. The adsorption of DODHPCA on steel surface leads to a physical barrier layer between the metal surface and the reaction environment inhibiting the charge transfer, and reduces corrosion reaction [39].

The values (ΔS_a) and (ΔH_a) accompanying the corrosion process were determined from the corresponding relation [39-41]:

$$r = \frac{RT}{Nh} \exp\left(\frac{\Delta S_a}{R}\right) \exp\left(\frac{-\Delta H_a}{RT}\right) \quad (12)$$

where h is Plank's constant 6.6261x10⁻³⁴ Js, N is Avogadro's number 6.0225x10²³ mol⁻¹, and R is the universal gas constant and T is the absolute temperature. Fig 11 shows the plots of $\log(r/T)$ versus $(1/T)$ for blank and inhibitor. From the values of the slope ($-\Delta H_a/2.303R$) and intercept [$\log(R/Nh) + (\Delta S_a/2.303R)$] of the linear plots, ΔH_a and ΔS_a , respectively are calculated, Table 5. It is noteworthy to say that, the positive sign of the ΔH_a implies that the dissolution of C-steel is endothermic process [40].

The values of entropy of activation (ΔS_a) with and without DODHPCA are negative, meaning that the activated complex in the rate-determining step represents an association rather than dissociation meaning that a decrease in disordering takes place on going from reactants to activated complex [42-44].

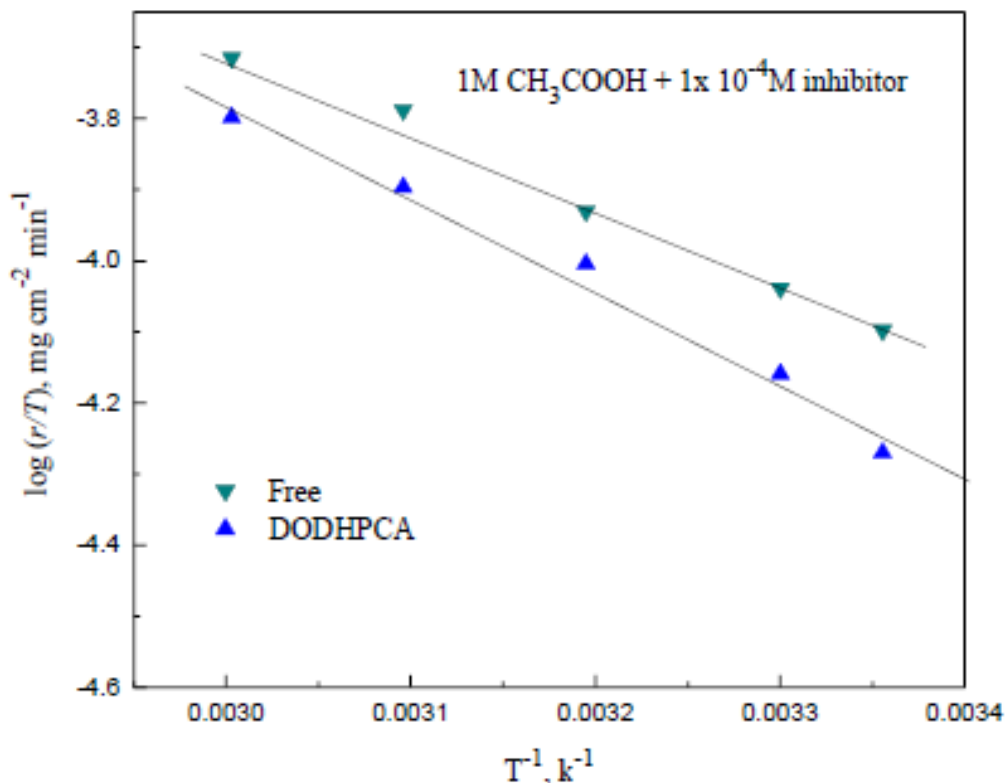


Figure 11. Transition state plots for C-steel in 1M CH₃COOH devoid of and containing 1 x10⁻⁴M inhibitor.

3.5. Adsorption isotherm

Different types of adsorption isotherms have been suggested to confirm the adsorption of DODHPCA on steel surface [51, 58, 59]. The experimental data obtained from mass loss method could confirm the Langmuir’s adsorption type according to the following forms [46].

$$\frac{\theta}{(1 - \theta)} = K_{ads} C_{inh} \tag{14}$$

$$\frac{C_{inh}}{\theta} = \frac{1}{K_{ads}} + C_{inh} \tag{15}$$

where the constant K_{ads} represents the adsorption equilibrium constant, and C_{inh} is the DODHPCA concentration at equilibrium state. Plotting the various values of (C_{inh}/θ) against the equilibrium concentration of DODHPCA, C_{inh} gives straight-line relation (Fig.12), confirming that the Langmuir adsorption model is the valid equation among the obtained experimental data. The validity of Langmuir adsorption isotherm is proved also from confirming the obtained value of the slope, which is very near to unity [26].

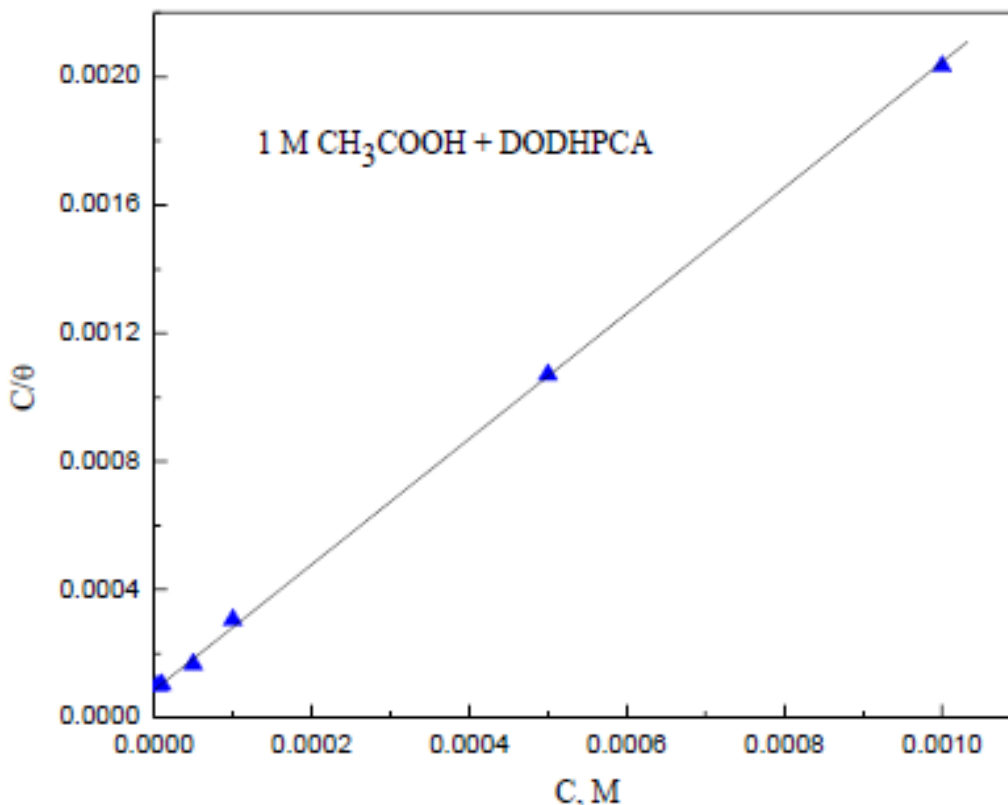


Figure 12. Langmuir adsorption isotherm (data from mass loss measurements).

The value of K_{ads} , could be calculated from the intercept of the straight line of Fig 12, is related to the standard free energy of adsorption, ΔG_{ads}° , in kJ mol^{-1} , according the equation [60-63]:

$$K_{ads} = \frac{1}{55.5} \exp\left(\frac{-\Delta G_{ads}^{\circ}}{RT}\right) \quad (16)$$

where 55.5 mol/l is the water concentration in the corrosive solution, $R = 8.314 \text{ J mol}^{-1} \text{ deg}^{-1}$ represents the gas constant and T is the adsorption equilibrium temperature in Kelvin scale. The calculated K_{ads} and ΔG_{ads}° adsorption parameters for DODHPCA are represented in Table 5.

Actually, the range of ΔG_{ads}° up to -20 kJ mol^{-1} are corresponding with the electrostatic interaction between the charged inhibitor molecule and the charged corrosive metal surface (physisorption) [26]. Values of ΔG_{ads}° between -40 and -400 kJ mol^{-1} are accompanying with chemical adsorption-type due to participation or transferring of electrons from the inhibitor molecules to form a coordinate bond with the metal surface [46-48]. The investigated inhibitor possess lone pair of electrons on each of N and O atoms, which can interact with d-orbitals of iron atoms on C-steel surface to form adherent barrier-film. The value of ΔG_{ads}° is $-33.1 \text{ kJ mol}^{-1}$, which is lower than -20 kJ mol^{-1} , but not as low as -40 kJ mol^{-1} or more, indicated that the adsorption mechanism of DODHPCA on C-steel surface in CH_3COOH solution was more than an electrostatic-adsorption, but not a true chemical-type [26]. The adsorption process may involve complex interactions involving both physical and

chemical adsorption of the inhibitor [39]. The negative value of $\Delta G^{\circ}_{\text{ads}}$ signifies a spontaneous adsorption of the inhibitor molecules beside the stability of the formed layer [49, 50]

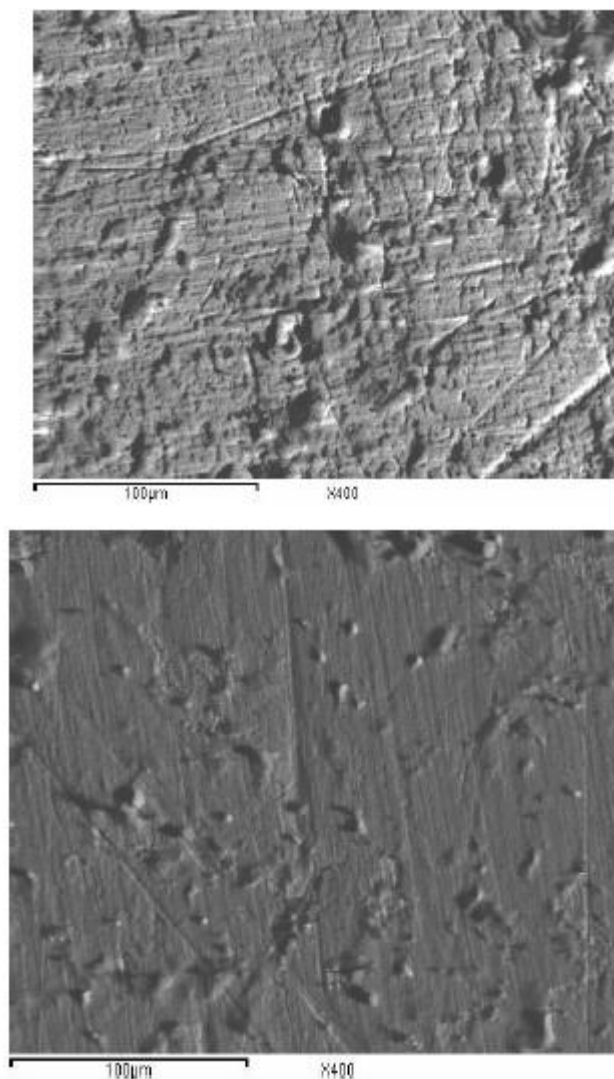


Figure 13A. SEM micrographs of C- steel after exposure time of 30 min, (a) in 1M CH_3COOH and (b) in 1 M $\text{CH}_3\text{COOH} + 1 \times 10^{-4}\text{M}$ inhibitor, at 25°C .

SEM micrographs shown in Fig. 13 (A&B) for C- steel are taken after 30 min immersion, at 25°C , in (A) 1M CH_3COOH and in (B) 1M $\text{CH}_3\text{COOH} + 1 \times 10^{-4}\text{M}$ DODHPCA. Investigation of the SEM micrograph taken in the corrosive solution without inhibitor explains that the C-steel surface was strongly damaged with laceration surface containing deep cavities containing corrosion products [51] (Fig. 13A). In presence of DODHPCA inhibitor, Fig (13B), the morphology of SEM shows less attacked surface compared with that of free acid[51]. This indicates that the presence of inhibitor hinders the dissolution of C-steel and thereby reduces the rate of corrosion revealing good protection against acid corrosion [52].

3.6. The inhibition mechanism

The inhibition of corrosion reaction of steel by DODHPCA was found to depend on the inhibitor concentration. The inhibition process depends on adsorption of the inhibitor at the electrode/solution interface [52, 53]. The nature of inhibitor interaction on metal surface during corrosion inhibition has been known from its adsorption characteristics [53, 54]. However, the inhibition efficiency ($\eta\%$) of inhibitor depends on many factors [53] which include the number of adsorption centers in the molecules, their charge density, molecular size, stability of the inhibitor on the metal surface, the mode of adsorption and formation of metallic complexes.

The corrosion inhibition of this compound towards the corrosion of C-steel in CH_3COOH may be attributed to the presence of a number of free electron pairs on hetero atoms and the conjugated π - bonds which are responsible for adsorb-ability of inhibitor on the attacked metal surface. The extent of the adsorption of an inhibitor depends on the nature of the metal, the mode of adsorption of the inhibitor, and the surface conditions[55]. Skeletal representation of the structure of the pyridinone derivative as an inhibitor for C-steel in CH_3COOH could be attributed to the presence of carbonyl group ($=\text{CO}-$) which has a lone pair of free electrons on O atom. Therefore, it acts as an electron-donating increases electron density on the adsorption site [56].

4. CONCLUSIONS

The study indicated that:

1. DODHPCA behaves as a mixed type of inhibitor for C-steel in acetic acid.
2. Inhibition effect increases DODHPCA concentration.
3. The adsorption of DODHPCA follows Langmuir model-type.
4. The inhibition of DODHPCA towards the corrosion of steel in CH_3COOH could be attributed to the adsorption through electron pairs on heteroatoms on metal surface.
5. The adsorption mechanism in CH_3COOH solution was an electrostatic-adsorption

References

1. M. B. Kermani and A. Morshed, *Corrosion NACE*, 59 (2003)659.
2. M. I. Alahmdi, S. Abd El Wanees, A. Ahmed Hathoot and Sabry Shaloot, *Woulfenia*, 22(2015) 116.
3. M. Abdallah, B.A. Al Jahdaly and O. A. Al-Malyo, *Int. J. Electrochem Sci.*, 10 (2015) 2740.
4. S. Sim, I.S. Cole, Y.-S. Choi and N. Birbilis, *Inter. J. Greenh. Gas Con.*, 29 (2014) 185.
5. M. A. Migahed, A. M. Al-Sabagh, E.A. Khamis and E.G. Zak, *J. Mol. Liq.*, 212 (2015) 360.
6. M.F. Morks, N.F. Fahim and T.H. Muster, I.S. Cole, *Surf. Coat. Technol.*, 228 (2013) 167.
7. P.C. Okafor and S. Nešić, *Chem. Eng. Commun.*, 194 (2007)141.
8. D. Liu, Z.Y. Chen and X.P. Guo, *Anti-Corros. Methods Mater.*, 55 (2008) 130.
9. G.A. Zhang and Y.F. Cheng, *Corros. Sci.*, 51 (2009) 1589.
10. M. N. El-Haddad and A.S. Fouda, *J. Mol. Liq.*, 209 (2015) 480.
11. D.A. Lo'pez, S.N. Simison and S.R. de Sanchez, *Corros. Sci.*, 47 (2005) 735.
12. M. Yadav, T.K. Sarkar and T. Purkait, *J. Mol. Liq.*, 212 (2015) 731.
13. M.A. Hegazy, I. Aiad and *J. Ind. Eng. Chem.*, 31(2015) 9199.
14. M. Abdallah, H.M. Al Tass, B.A. Al Jahdaly and A.S. Fouda, *J. Mol. Liq.*, 216 (2016)590.

15. M. Abdallah, B. A. Al Jahdaly, M. Sobhi and A. I. Ali, *Int. J. Electrochem. Sci.*, 10 (2015) 4482.
16. M. Abdallah, A. M. El-Dafrawy, M. Sobhi, A. H. M. Elwahy, and M. R. Shaaban, *Int. J. Electrochem. Sci.*, 9 (2014) 2186.
17. S. A. Umoren and U. M. Eduok and *Carbohydr. Polym.*, 140 (2016) 314.
18. S. A. Odoemelum, N.O. Eddy and *J. Mater. Sci.*, 4 (2008) 87.
19. M. Sobhi, R. El-Sayed and M. Abdallah, *J. Surfactants Deterg.*, 16(2013) 937.
20. H. Ashassi-Sorkhabi, B. Shaabani and D. Seifzadeh, *Electrochim. Acta*, 50 (2005) 3446.
21. S.M. Abd El Haleem, S. Abd El Wanees, E.E. Abd El Aal and A. Diab, *Corros. Sci.*, 52(2010)1675.
22. M. Abdallah, A. I. El Zaafarany, S. Abd El Wanees and R. Assi, *Int. J. Corros. Scale Inhib.*, 4 (2015) 338.
23. S.M. Abd El Haleem, S. Abd El Wanees, E.E. Abd El Aal and A. Farouk, *Corros. Sci.*, 68 (2013) 1.
24. S. Abd El Wanees and E.E. Abd El Aal, *Corros. Sci.*, 52 (2010) 338.
25. S.M. Abd El Haleem, and S. Abd El Wanees, *Mater. Chem. Phys.*, 128(2011) 418.
26. S. Abd El Wanees, A. Diab, O. Azazy and M. Abd El Azim, *J. Dispersion Sci. Techn.*, 35 (2014) 1571.
27. J.O'M Bockris and D.A.J. Swinkels, *J. Electrochem. Soc.*, 111 (1964) 736
28. N. A. Negm, E. A. Badr, I.A. Aiad, M.F. Zaki and M. M. Said, *Corros. Sci.*, 65 (2012) 77.
29. L. Vrsalović, S. Gudić, M. Kliškić, E. E. Oguzie, L. Carev and L. Carev, *Int. J. Electrochem. Sci.*, 11 (2016) 459.
30. S.M. Abd El Haleem, S. Abd El Wanees, E.E. Abd El Aal and A. Farouk, *Corros. Sci.*, 68 (2013) 14.
31. W. Li, Q. He, S. Zhang and B. Hou, *J. Appl. Electrochem.*, 38 (2008)289.
32. L. Afia, R. Salghi, Eno. E. Ebenso, M. Messali, S. S. Al-Deyab and B. Hammouti, *Int. J. Electrochem. Sci.*, 9 (2014) 5479.
33. M. A. Hegazy, A. S. El-Tabei, A. H. Bedair and M. A. Sadeq, *RSC Adv.*, 5 (2015) 64633.
34. E. A. Noor, *Int. J. Electrochem. Sci.*, 2(2007) 996.
35. M. A. Amin, S. S. Abd El-Rehim, E.E. F. El-Sherbini, and R. S. Bayoumi, *Int. J. Electrochem.*, 3 (2008) 199.
36. J. Yu and F. Gan, *Anti-Corros. Methods Mater.*, 55 (2008)257.
37. H. A Mohamed and M. H. Abdel Rehim, *Anti-Corros. Methods Mater.*, 62 (2015) 95.
38. M. Abdallah, S. T. Atwa and A. Zaafarany, *Int. J. Electrochem. Sci.*, 9 (2014) 4747.
39. B.S. Sanatkumar, Jagannath Nayak and A. Nityananda Shetty, *Inter. J. Hydr. Energy*, 37(2012) 9431.
40. S. Martinez and I. Stern, *Appl. Surf. Sci.*, 199(2002)83.
41. I. N. Putilova, S. A. Balezin and U. P. Baranik, *Metallic Corrosion inhibitor* (1960), Pergamon Press, New York, p 31.
42. A. Abdel-Nazeer, N. K. Allam, A.S. Fouda and E.A. Ashour, *Mater. Chem. Phys.*, 136 (2012)1.
43. M. Behpour, S. M. Ghoreishi, M. Khayatkashani and N. Soltani, *Corros. Sci.*, 53(2011) 2489.
44. M. Boukalah, B. Hammouti, M. Lagrenee and F. Bentiss, *Corros. Sci.*, 48(2006) 2831.
45. I. Lukovists, E. Kalman and F. Zuchi, *Corrosion NACE*, 57 (2001) 3.
46. S.M. Abd El Haleem, S. Abd El Wanees, and A. Baghat, *Corros. Sci.*, 78 (2014)321.
47. B. Berka-Zougali, M. A. Ferhat, A. Hassani, F. Chemat, and K.S. Allaf, *Int. J. Mol. Sci.*, 13 (2012) 4673.
48. Shi, X. Wang; J. Yu and B. Hou, *Anti-Corros. Methods Mater.*, 58 (2011) 111.
49. M.M. Solomon, S.A. Umoren, I.I. Udoso and A.P. Udoh, *Corros. Sci.*, 52 (2010) 1317.
50. S. A. Umoren and U. F. Ekanem, *Chem. Engin. Commun.*, 197(2010) 1339.
51. A. Khamis, M. M. Saleh, M. I. Awad and B.E. El-Anadouli, *Corros. Sci.*, 74(2013)83.
52. H. B. Rudresh and S. M. Mayanna, *J. Environ. Sci. Technol.*, 122 (1977) 25.
53. A.S. Fouda, G.E. Badr and M.N. El-Haddad, *J. Korean Chem. Soc.*, 52 (2008) 124.

54. T. Murakawa, T. Keto, S. Nagura and N. Hackerman, *Corros. Sci.*, 8 (1968) 438.
55. I.B. Obot, N.O. Obi-Egbedi and S.A. Umoren, *Int. J. Electrochem. Sci.*, 4 (2009) 863.
56. B.A. Abd-El-Nabey, A.M. Abdel-Gaber, G.Y. Elewady, M.M. El. Sadeek and H. Abd-El-Rhman, *Int. J. Electrochem. Sci.* 7 (2012) 11718.

© 2016 The Authors. Published by ESG (www.electrochemsci.org). This article is an open access article distributed under the terms and conditions of the Creative Commons Attribution license (<http://creativecommons.org/licenses/by/4.0/>).